



Spatial variability of the urban ground motion in a highly heterogeneous site-city configurations

C. Varone¹ · L. Lenti^{2,5} · S. Martino³ · J. F. Semblat⁴

Received: 6 March 2020 / Accepted: 18 September 2020 / Published online: 15 October 2020
© Springer Nature B.V. 2020

Abstract

Free-field conditions on the ground surface are widely used to assess the local seismic response. Nevertheless, this assumption is a very strong approximation in urban areas since the dynamic interaction between the urban agglomerate and the soil cannot be neglected. Several studies evidenced the transmission of vibrations from the buildings to the soil and the multiple interactions between a building network and the site through so-called Site-City Interaction (SCI). This paper focuses on the spatial variability of the seismic ground motion due to SCI in the case of highly heterogeneous site-city configurations. The Fosso di Vallerano valley in Rome (Italy) has been chosen as a case study because of the high heterogeneity of the deposits which characterize the local geological setting as well as the intensive urbanization. A proper 2D numerical modelling (Finite Elements Method) of the seismic response in free-field conditions as well as with the city agglomerates (SCI-based condition) has been performed. The numerical results show a strong spatial variability of the wave field induced by the presence of the buildings and their interaction with the heterogeneous soil. The SCI effect causes a strong or global reduction of ground motion, amplification levels and kinetic energy close to the buildings. Induced perturbations affect the ground motion along the surface of the model, increasing the amplification values and the kinetic energy in the vicinity of the buildings. These findings highlight that buildings generate significant variability effects all around their foundations as well as in the entire alluvial basin.

Keywords Wave propagation · Site-City Interaction · Spatial variability · Local seismic response · Numerical modelling

Electronic supplementary material The online version of this article (<https://doi.org/10.1007/s10518-020-00965-2>) contains supplementary material, which is available to authorized users.

✉ C. Varone
chiara.varone@igag.cnr.it; chiara.varone@cnr.it

Extended author information available on the last page of the article

1 Introduction

Strong earthquakes have recently affected densely urbanized areas, leading to a high level of urban destruction: Italy 2009 ($M_L \approx 5.9$), Haiti 2010 ($M_W \approx 7.0$), Chile 2010 ($M_W \approx 8.8$), New Zealand 2011 ($M_L \approx 6.3$), Nepal 2015 ($M_L \approx 7.8$) and Italy 2016 ($M_L \approx 6.0$). These areas are diffusely built in complex geological contexts, responsible for various seismic site effects. Local heterogeneity of the subsoil causes vertically and horizontally seismic impedance contrasts due to the different mechanical properties of the alluvial deposits in urban areas (i.e. basins, valleys, and canyons). Such site effects derive from physical phenomena such as 1D resonance (Dobry and Vucetic 1987), seismic-wave interaction with 2D basins (Bard and Bouchon 1985), generation of surface waves (Semblat et al. 2010; Narayan 2010; Meza Fajardo et al. 2016, 2019) and the focusing of seismic waves related to peculiar basin shapes (Gao et al. 1996; Booth et al. 2004; Narayan 2012; Narayan and Kumar 2014, Semblat et al. 2002, Licata et al. 2019).

Moreover, perturbations of the ground motion, compared to the ones expected under free-field conditions, can be observed in urban areas as consequence of the presence of the buildings acting as secondary source (Guéguen et al. 2000, 2002). In this regard, the presence of several structures in the urbanized areas generates multiple Structure-Soil-Structure Interactions (SSSI according to Luco and Contesse 1973; Wong and Trifunac 1975), known in literature as “Site-City Interactions SCI” (Guéguen et al. 2002; Fernández-Ares and Bielak 2004; Bard et al. 2005; Kham et al. 2006; Semblat et al. 2008).

The main goal of the present research is to assess the spatial variability of the seismic ground motion due to SCI for highly heterogeneous subsoils in urban areas through numerical approaches. At this aim, the Fosso di Vallerano valley, SE of Rome (Italy), was selected because of its very complex geological setting (highly heterogeneous soil deposits) synthesized in a high-resolution geological model defined by Bozzano et al. 2015. Additionally, it has recently experienced urban expansion, which completely perturbed the free-field conditions of the original alluvial valley from the tributaries of the Tiber River during the Holocene. The progressive urbanization of this area over the last decade was reproduced in the numerical computations (detailed buildings models). The existing buildings designed and built at different periods are composed of various materials. Full 2D FEM-based numerical simulations assuming free field and SCI conditions are performed to assess the influence of buildings on the local seismic response. The spatial variation of the main physical properties of the seismic waves (e.g. spatial propagation, amplification levels, ground kinetic energy) for both the free and the urban wave field are derived to evaluate the influence of such an irregular city on the ground motion.

2 Site–City interaction: state of the art

SCI includes the combined effects of subsoil geology, kinematic and inertial Soil-Structure Interactions (SSI) at a global scale (Bard et al. 2005). Since the end of the 1990s, several authors (Wirgin and Bard, 1996; Tsogka and Wirgin, 2003; Kham et al. 2006; Semblat et al. 2008; Taborda and Bielak 2011a, b; Hori et al. 2018; Kumar and Narayan 2018, 2019, Ungureanu et al. 2019) performed 2D and 3D numerical simulations to evaluate the influence of urban agglomerates on the seismic wave field when compared to the free-field condition. Clouteau and Aubry (2001) and Clouteau et al. (2002) performed 3D numerical

modelling through a boundary-element method (BEM) to evaluate the SCIs in Nice, France, and Mexico City. Isbiliroglu et al. (2015) simulated SCIs in the San Fernando valley during the 1994 Northridge earthquake.

Other authors studied SCI through analytical approaches: Guéguen et al. (2002) described the global city effects of urban agglomerates by adding the contribution from a series of single oscillators to represent the buildings, and Boutin and Roussillon (2004) focused on multiple interactions between buildings using homogenization methods.

Some physical experiments were performed by Guéguen et al. (2000) and Gueguen and Bard (2005) analyzing a reduced-scale structure at the Volvi EuroSeist Test site while Galipoli et al. (2006) considered buildings as a seismic source in a test site in Italy. These studies pointed out that the effects of SCI on the ground motion strongly depend on the urban configuration as well as the heterogeneity of building density and typology; nevertheless, in these studies the influence of seismic site effects on SCI was simplified (e.g. by assuming homogeneous alluvia). The numerical results obtained so far are mainly focused on theoretical urban configurations composed of homogeneous buildings, usually modelled as oscillators and/or equivalent homogeneous structures. On the contrary, the here proposed study focuses on a heterogeneous city model to analyze the SCI in an highly heterogeneous alluvial valley.

3 Heterogeneous geological setting of the Fosso di Vallerano valley

The Fosso di Vallerano valley exhibits a complex geomorphological setting because of a complex evolution linked to the Würmian glacio-eustatic cycle, which led to a sequence of successive deviations and rearrangements of the riverbed (Ascani et al. 2008).

According to Bozzano et al. (2016) five main litho-stratigraphic groups can be distinguished in the geological setting of the alluvial valley:

- Plio-Pleistocene marine sediments (Marne Vaticane, Monte Mario and Monte Ciocci/delle Piche Formations), which represent the geological bedrock (PP);
- Pleistocene alluvial sediments deposited by the Paleo-Tiber 4 River (Santa Cecilia Formation; MIS 15; 650–600 ka; Marra and Florindo 2014) (PT): clays and silts with peaty layers (PT-CL), sands and silty sands. (PT-SD), loose gravels with sedimentary components (PT-GR).
- Volcanic deposits that erupted from the Alban Hills and the Monti Sabatini volcanic district (561–365 ka; Karner et al. 2001) (VC) (RED and VSN in Fig. 1);
- Pre-Würmian fluvio-palustrine deposits (500–200 ka; Karner and Marra 1998) (FP) (TDC, VTN, FTR, VGU in Fig. 1);
- Recent alluvial deposits that filled the valley incisions since the end of the Würmian regression to the present (MIS 1; 18 ka-present; Marra et al. 2013) (AL): anthropic filling material (AL-FA), sandy-clays with volcanic component (AL-VSC), peaty clays (AL-PC), clays and silts (AL-CL/AL-LS(CL)), peat (AL-PT), 6) sands and silty sands (AL-SD), gravels with volcanic and sedimentary components (AL-GR/AL-LS(GR)) (SFT in Fig. 1).

A syn-sedimentary tectonic activity dislocated the geological bedrock (PP units) and the overlying PT deposits, leading to a horst and graben structure (Bozzano et al. 2016). The presence of these buried tectonic structures and of strong horizontal and vertical

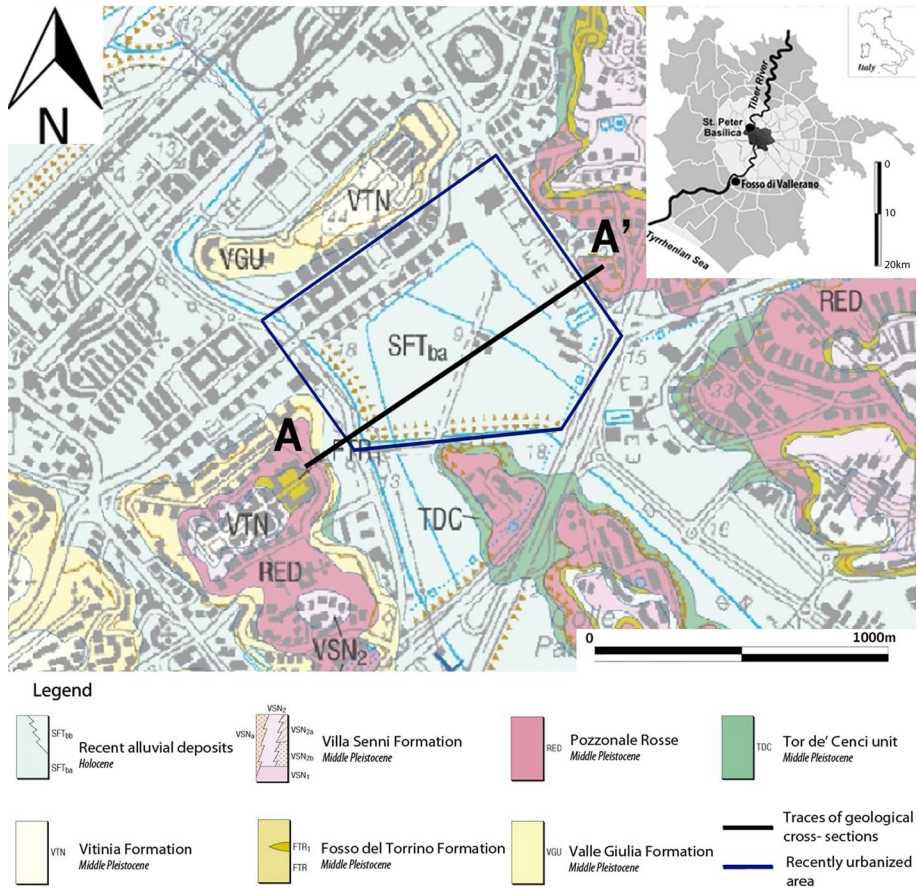


Fig. 1 Geological map of the Fosso di Vallerano area from Funicello and Giordano (2008). The trace of the geological cross-section AA' and the area interested by the urban development are also reported

heterogeneities determines the presence of strong seismic site effect in the Rome area (Rovelli et al. 1995; Bozzano et al. 2008, 2012, 2017; Alessi et al. 2014, Martino et al. 2015, Varone et al. 2016). Several geological cross sections were proposed by Bozzano et al. (2016) to reconstruct the 3D model of the Fosso di Vallerano valley. The geological cross section along traces AA', displayed in Fig. 1, is considered in this study (see Online Appendix 1 for soil model geometry).

The Fosso di Vallerano valley hosts a modern district of Rome where dense urban agglomerates have been widely developing over the last decades. In particular, the urbanization of the study area began in 2002 with the building up of an urban complex including residential reinforced concrete buildings. These buildings are mainly characterized by a regular base and they are composed of 6–9 floors. The urban expansion evolved southward including new residential, commercial and institutional buildings.

This urbanization has been planned in the “Europarco Business Park” project, which includes a total of 10 buildings including the Italian Ministry of Health, one of the largest shopping centers in Rome (Euroma 2) and two skyscrapers (Euroskey and Europarco towers), which currently are the tallest buildings in Rome.

4 Modelling assumptions

The numerical modelling was carried out in the framework of the Finite Element Method (FEM) through time domain integration (CESAR-LCPC code, Humbert et al. 2005). The engineering-geological model proposed by Bozzano et al. (2015, 2016) was discretized in terms of finite elements and a linear viscoelastic behavior is assumed for the modelled deposits whose parameters values are summarized in Table 1.

The model was discretized in three-noded linear elements calibrated on the minimum wavelength in the models so limiting numerical dispersion. As reported by Semblat and Pecker (2009), the element size strongly influences the numerical error. Numerical dispersion from coarse mesh can under-estimate the amplitude and over-estimate the velocities. This factor can be reduced by choosing a suitable element size Δh with respect to the wavelength of the problem (1):

$$\Delta h = \frac{\lambda}{11} \quad (1)$$

where λ = wavelength and Δh = element size.

Element sizes of 1 m in the first case and 10 m in the second case were chosen to solve the problem up to a frequency of 10 Hz according to the lowest S-wave velocity of the alluvial deposits (118 m/s) and the largest velocity (1100 m/s) for the seismic bedrock and the absorbing layer system.

A Rayleigh-type damping was considered according to the following relation:

$$[C] = a[K] + b[M] \quad (2)$$

where $[C]$, $[M]$, $[K]$ are the viscosity, mass and stiffness matrices respectively and a and b are the Rayleigh constants controlling the frequency dependence of the damping ratio.

A 150 m thick seismic bedrock (NM in Table 1) was modelled at the bottom of each section in the alluvial deposits. According to Semblat et al. (2011), a set of heterogeneous absorbing layers based on Rayleigh/Caughey damping formulation (CALM) placed at the lateral and bottom boundaries of the models may avoid spurious wave reflections at the boundaries of the numerical model. The absorbing layers system consists of 5 sub-layers with a damping value ranging linearly from $Q_{\min}^{-1} \approx 0.20$, or $\xi = 0.10$ (in the inner portion of the model), to $Q_{\min}^{-1} \approx 2.00$, or $\xi = 1.00$ (at the extreme lateral boundary of the model) (Varone et al., 2014).

The models were excited by natural earthquakes recorded by a seismometric array installed in Fosso del Vallerano from June to July 2009 (Bozzano et al. 2016) and by a synthetic Oth-order Ricker wavelet (Ricker 1943, 1953), applied as a horizontal displacement with a PGD (Peak Ground Displacement) normalized to 1 m and a frequency content from 0.1 to 15 Hz. For the purpose of this manuscript, considering that the results are non-sensitive to the input typology, only the findings obtained by the synthetic wavelet are presented. The models have been computed considering an in-plane motion propagating upward from the bottom of the model.

5 Structural and dynamic characterization of the buildings

A preliminary characterization of the buildings from a structural point of view was performed to evaluate the dynamic behaviour in terms of modal properties, particularly the first eigenmode of each building for the following numerical SCI-based simulations. In

Table 1 Viscoelastic properties of the various materials modeled

| Lithological units | ID | ρ (kg/m ³) | V_s (m/s) | V_p (m/s) | ν | G (MPa) | E (MPa) | ξ (%) strain = 0.001% | b (1/s) | a (s) |
|--------------------|-------|-----------------------------|-------------|-------------|-------|---------|---------|------------------------------|---------|----------|
| AL-FA | 1 | 1732.9 | 118.3 | 221.3 | 0.30 | 24.3 | 60.6 | 1 | 0.5027 | 1.99E-04 |
| AL-VSC | 2 | 1682.0 | 225 | 420.9 | 0.30 | 85.1 | 212.9 | 1 | 0.5027 | 1.99E-04 |
| AL-CP | 3 | 1753.3 | 150 | 280.6 | 0.30 | 39.4 | 98.6 | 3 | 1.2252 | 7.35E-04 |
| AL-CL | 4 | 1865.4 | 235 | 439.6 | 0.30 | 103.0 | 257.5 | 2 | 1.0053 | 3.98E-04 |
| AL-PT | 5 | 1294.6 | 140 | 261.9 | 0.30 | 25.4 | 63.4 | 1 | 0.5027 | 1.99E-04 |
| AL-SD | 6 | 1957.2 | 417 | 780.1 | 0.30 | 340.3 | 850.8 | 1 | 0.5027 | 1.99E-04 |
| AL-GR | 7 | 2140.7 | 713 | 1333.9 | 0.30 | 1088.3 | 2720.6 | 1 | 0.5027 | 1.99E-04 |
| VC | 8 | 1834.9 | 1100 | 1905.3 | 0.25 | 2220.2 | 5550.5 | 1 | 0.5027 | 1.99E-04 |
| AL-LS (AR) | 9 | 1865.4 | 250 | 467.7 | 0.30 | 116.6 | 291.5 | 3 | 1.2252 | 7.35E-04 |
| PT-SD | 10 | 1957.2 | 417 | 780.1 | 0.30 | 340.3 | 850.8 | 1 | 0.5027 | 1.99E-04 |
| PT-CL | 11 | 1865.4 | 357 | 667.9 | 0.30 | 237.7 | 594.4 | 3 | 1.2252 | 7.35E-04 |
| PT-GR | 12 | 2140.7 | 1100 | 2057.9 | 0.30 | 2590.2 | 6475.5 | 1 | 0.5027 | 1.99E-04 |
| NM | 13–14 | 2140.7 | 1100 | 1905.3 | 0.25 | 2590.2 | 6475.5 | 0.5 | 0.2042 | 1.22E-04 |

ID = Lithological unit identification code, ρ = density, V_s = S-waves velocity, V_p = P-waves velocity, ν = Poisson coefficient, G = Shear modulus, E = Young modulus, ξ = damping ratio, b/a = Rayleigh constants

this identification, buildings were modelled in the two-dimensional plane as stand-alone structures, i.e. without taking into account SSI and SSSI.

Most of these buildings were built in the last decades and are residential ones, i.e. characterized by a reinforced concrete structure and a shallow foundation. The two skyscrapers of the Europarco Business Park are characterized by a mixed bearing structure of steel and reinforced concrete (Colombo 2012). In particular, beams and shallow foundations are characterized by steel structure, while columns are reinforced concrete members. Additionally, these structures have deep foundations that are linked to the raft with a thickness of 6 m; the piles are reinforced concrete structures. The design features of the buildings, summarized in Table 2 (see Online Appendix 2 for more details), are taken into account to simulate the dynamic behaviour of the modelled buildings.

Each structure was modelled according to its super-structures (Fig. 2); in particular, all the beams, columns and shallow foundations are modelled as solid elements. It is worth noticing that the buildings were not modelled as homogeneous equivalent solids to avoid unrealistic wave focusing at some specific locations. The solid elements were discretized by three-noded linear elements, and the buildings are clamped at their base.

The thickness of the shallow foundation is 1 m for all the buildings except for the skyscrapers, for which the thickness of the foundation is 6 m. The pile foundations were modelled by assuming a Timoshenko beam (Oñate 2003) with a diameter of 1.2 m and a length of 60 m for each pile. The beam-to-column junctions have been considered as perfectly stiff (only horizontal movements are allowed, and rotation and bending are prevented). The elastic modulus assumed are 30 GPa for reinforced concrete and 210 GPa for the mixed material composed of steel and reinforced concrete. A linear viscoelastic behavior is assumed for the modeled structures by Rayleigh-type damping with $\xi = 0.05\%$ at strain = 0.001%. The first eigenmode of each building (Table 2) was evaluated through FEM based modal analysis and corresponds to in-plane bending, while out-of-plane bending were not simulated. To simulate the increasing urbanization of the valley along the modelled section AA' of Fig. 1, two different distribution of buildings (TA1-2006, TA2-2011 for section AA') were considered, representing the progressive evolution of the urban configuration over time starting from the free field conditions.

Table 2 Geometrical and structural features of the modelled buildings (cf. map in Fig. 2)

| Building ID | Height (m) | Type of foundation | Type of bearing structure | First eigenfrequency (Hz) |
|--------------------------|------------|--------------------|-----------------------------|---------------------------|
| <i>Cross section AA'</i> | | | | |
| 1 | 24 | Shallow foundation | Reinforced concrete | 4.1 |
| 2 | 120 | Deep foundation | Steel + reinforced concrete | 0.5 |
| 3 | 33 | Shallow foundation | Reinforced concrete | 3.8 |
| 4 | 120 | Deep foundation | Steel + reinforced concrete | 0.5 |
| 5 | 6 | Shallow foundation | Reinforced concrete | 20 |
| 6 | 7 | Shallow foundation | Reinforced concrete | 36 |

The fundamental resonance frequency of each building is also reported

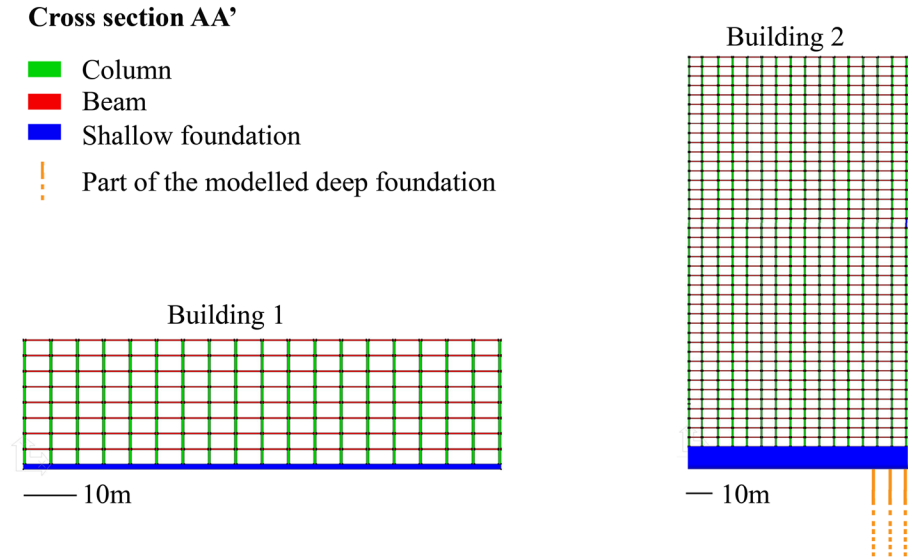


Fig. 2 Examples of building models. Piles foundations are partially represented (out of scale) for building 2. See Sect. 5 for details about piles

6 Assessment of the seismic ground motion in the basin

The Wave Propagation Map (WPM) along the surface of the model considering free field conditions (Fig. 3a) enables to analyse waves reflection and refraction due to the shape of the valley and to verify the efficiency of the absorbing layer system. All the WPM show the displacement distribution along the surfaces of the models in the first 5 s for which the ground motion is meaningful. The WPM for the horizontal and vertical displacement show that different wave arrivals may be noticed along the valley (central portion for the model AA') probably due to both the heterogeneity of the alluvial filling and the shape of the valley (Fig. 3a).

At the outcropping bedrock (left and right sides of the AA') no significant wave refraction or reflection occurs. The analysis of the displacement at the boundary and within the CALM area (Fig. 4) highlights the efficiency of the absorbing layer system for all sides of the FE mesh. Within the first 300 m of the CALM system, all the waves are damped, and no displacement is observed.

The numerical results were also analyzed in terms of amplification functions $A_x(f)$ (Borchedt 1970, 1994) along the valley, computed as spectral ratio between the horizontal component of all the grid-nodes along the domain surface and the horizontal component of the signals on the seismic bedrock. The values are averaged for neighboring nodes.

The $A_x(f)$ functions were interpolated through a Kriging regression and displayed as contour maps under different conditions. An analysis of the $A_x(f)$ (Fig. 5a) obtained for AA' profile highlighted the non-homogeneous distribution of the amplification peaks along the valley.

The first peak ranges from 0.8 to 1.2 Hz according to the 1D stratigraphic resonance of the alluvia. These results agree with experimental results obtained from ambient noise measurement reported by Bozzano et al. (2016). Higher order modes appear because of the thin heterogeneities along a section. The results obtained for the Fosso di

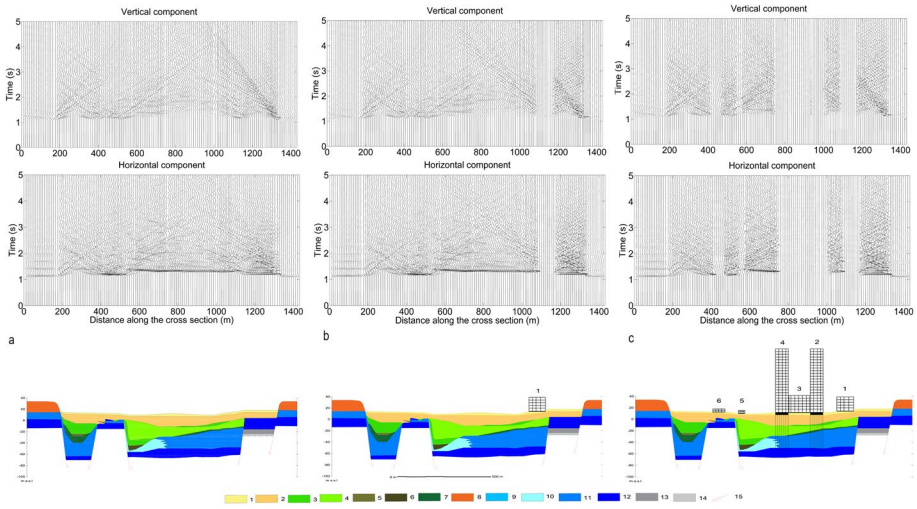


Fig. 3 WPM of the vertical and horizontal components of the displacement along the AA' (free field, left), TA1 (urban wave field n.1, middle) and TA2 (urban wave field n. 2, right) models surface. See Table 1 for geological legend

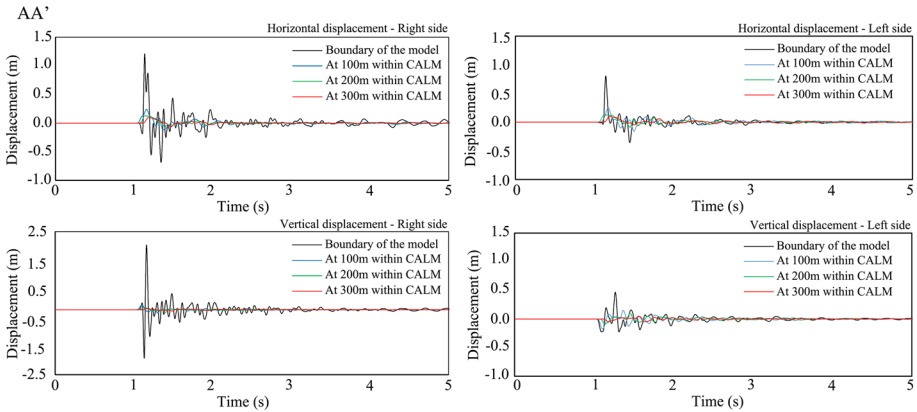


Fig. 4 Displacement at the transition and within the absorbing layer system (CALM) of AA' model surface

Vallerano test site herein highlight that the presence of a tectonic structure like a horst in the middle of the valley, induces amplification effects at frequencies that are usually not amplified. Therefore, impedance contrasts related to lateral heterogeneities as well as bedrock shape cannot be neglected to assess a more reliable $A_x(f)$ as already demonstrated for the Rome’s city center by Martino et al. (2015).

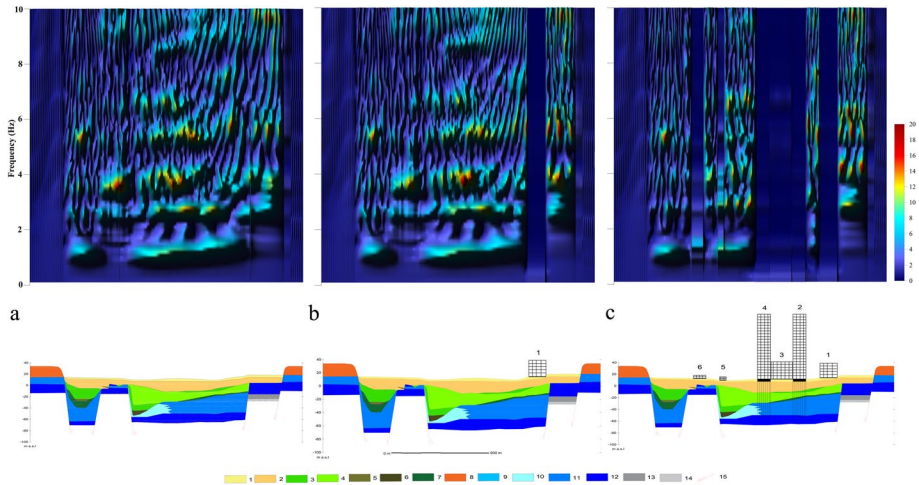


Fig. 5 Contour map of the $A_x(f)$ functions distribution along the AA' (free field, left), TA1 (urban wave field n.1, middle) and TA2 (urban wave field n. 2, right) models' surface. See Table 1 for geological legend

7 Site-city configurations

7.1 Various urban configuration

The progressive development of the urban agglomerate in the geological cross section was modelled to evaluate the progressive influence of the buildings on the local seismic response of the valley with respect to free-field conditions considering their contribution in the plain of the simulation. Each building is first characterized from a structural perspective, and the dynamic behavior is modelled to derive the first eigenmode. They are inserted into the free-field FEM models according to their super-structures, i.e., all the bearing structures simulated during the previous phase. The boundaries of super-structures elements coincide with the soil interface, which implies perfect bonding between the structures and the soil (SSI assumption: continuity of displacement). The geological cross section (previously modelled under free-field conditions) is progressively populated with buildings according to the urban development of the Fosso di Vallerano valley. Consequently, it defines the main urbanization steps of the analyzed cross section. A 125 m wide representative geological cell within which the geological section is representative, is defined. The buildings in the cells are considered to define the various urbanization steps. The models representing the urban development steps (years) are defined as follows:

- cross section AA': TA1 = 2006 (Fig. 3b); TA2 = 2011 (Fig. 3c).

The parameters for the geological filling, the mesh sizes and the boundary conditions are presented in Sect. 4, while the parameters and the mesh sizes for the buildings are shown in Sect. 5. All the coupled models are excited by the seismic inputs introduced in Sect. 4.

7.2 Assessment of the local urban seismic motion

The WPM of the horizontal and vertical displacement along the surfaces of the coupled models (AA' in Fig. 3b, c) show the influence of the urbanization on the ground motion with respect to the free-field conditions. The effect of buildings is combined with the influence of the subsoil geology. Compared to the free field conditions, two additional effects due to the presence of the buildings may be identified: (1) the presence of buildings with small volumes and masses (e.g., buildings 5–6 in AA' coupled models), which strongly reduce the ground motions close to the foundations of these buildings; (2) the presence of buildings with larger volumes and masses (e.g., building from 1 to 4 in AA' coupled models), which induces negligible ground motion at the foundation level. The presence of buildings also increases the duration of the ground motion with respect to free-field conditions. The distribution of $A_x(f)$ values along the AA' coupled models (Fig. 5b, c) highlights a very complex spatial distribution of the amplifications. The presence of the buildings induces an increase of the spatial variability of the amplification levels (Fig. 5b, c) if compared to the free field conditions (Fig. 5a). It appears different for the two buildings typologies. In particular, the presence of buildings with small volumes and masses (e.g., buildings 5–6 in AA' coupled models) leads to an additional amplification peak in the frequency range 0.8–1.2 Hz that was not observed in the free-field case. The resulting amplification peaks close to the buildings with larger volumes and masses (e.g., building 1 in the TA1 model in Fig. 5b) disappears and no seismic amplification effects are observed. Conversely, the portions of the valley that surround the buildings are characterized by higher numbers of amplification peaks and a larger amplification level for each peak.

8 Spatial variability of the urban seismic ground motion

8.1 Spatial distribution of the kinetic energy

To assess the spatial variability of the urban ground motion, the ground motion energy distribution along the surface of the model is evaluated through the formulation (3) proposed by Kham et al. (2006):

$$E(x) = \frac{1}{T} \int_0^T \left[\frac{du}{dt}(x, t) \right]^2 dt \quad (3)$$

where T is the signal duration, u is the displacement, and t is the time.

The ratios between $E(x)$ distributions for the coupled models (Fig. 3b, c) and the corresponding free-field models (Fig. 3a) were computed to quantify the influence of buildings on the kinetic energy along the ground surface. The variation in the ratios along the surfaces of the models (Fig. 6) show that the buildings strongly reduced the $E(x)$ value in comparison with the free field condition. The reduction in the kinetic energy close to the buildings is in agreement with the results by Kham et al. (2006) who discuss that, such a reduction is controlled by two factors: the ratio between the soil and building frequencies (the closer these frequencies, the larger the reduction), and the building density (the greater the building density, the larger the decrease). For the Fosso di Vallerano case study, it results that the spatial variability of cumulated kinetic energy is controlled, rather than

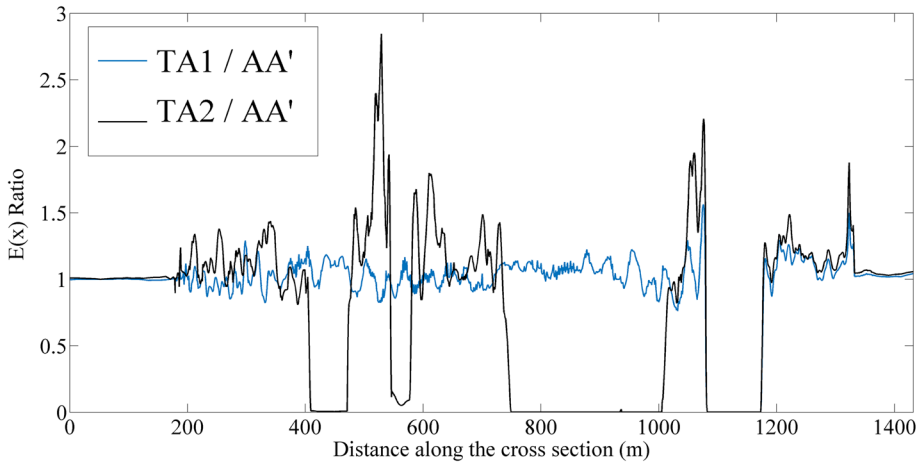


Fig. 6 Ratio between the kinetic energy $E(x)$ index considering SCI and free field conditions along the AA' models surface

by the frequency match between the soil and building, by the buildings density and by the typologies of dynamic SSI, i.e. kinematic and inertial interactions. This reduction is more intense close to the buildings with smaller volumes and masses (i.e., buildings 5–6 of TA2 model in Fig. 3c) while it is maximum where the buildings are characterized by greater volume and mass (i.e., building 1 of TA1 model in Fig. 3b). Both kinematic and inertial interactions affect the SSI and SCI, even if distinguishing these effects, it is not well constrained. Buildings with large volumes and masses should induce a predominance of inertial interactions with respect to kinematic interactions. This effect completely nullifies the ground motion, seismic amplification levels and kinetic energy close to the buildings because of the inertial forces that are generated at the soil–foundation interface. Buildings with small volumes and masses, i.e., structures with lower inertia, should increase kinematic interactions with respect to the previous case (i.e. buildings with large volumes and masses). The more the dynamic SSI is characterized by an inertial component, the less the reduction on the cumulated kinetic interaction results. The areas surrounding the buildings are characterized by an increase in the kinetic energy (Fig. 6). In particular, the $E(x)$ ratio reached 2.8 (Fig. 6), indicating a kinetic energy level 2.8 times higher than the corresponding energy under free-field conditions at the same location. This kinetic energy increase is not uniformly distributed along the non-urbanized portions of the area and strongly increased in the central portion of the TA1 and TA2 models, i.e., the areas characterized by the most complex geological settings so indicating a strong influence of the geological setting. The more heterogeneous is the subsoil, the larger is the increase of cumulated kinetic energy.

8.2 Assessment of the seismic amplification

To quantify the influence of SCI on new constructions, the response spectra (Fig. 7) along the valley are calculated (Points 1A and 2A in Fig. 8). The analysis of the normalized response spectra (Fig. 7) highlights that response spectra in unbuilt areas are influenced by the buildings in the surroundings. Such an influence is distributed in a wide period range (0.0–0.5 s) and an

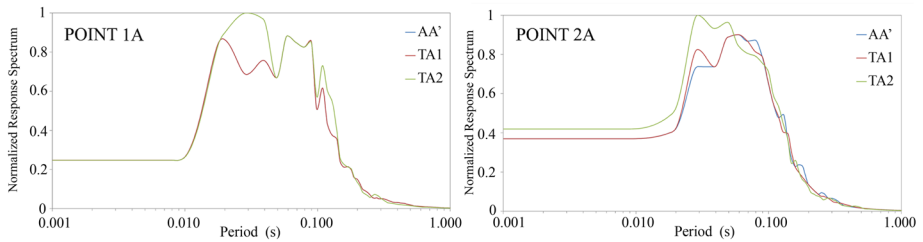


Fig. 7 Normalized response spectrum at point 1A and 2A along AA', TA1, TA2 models. See Figures 12 and 13 for the location of the points

Table 3 Amplification factors values computed for the most relevant points along the modelled sections AA' at different urbanization steps

| Urban development | Point | AF (0.1–0.5 s) | AF (0.4–0.8 s) | AF (0.8–1.1 s) |
|--------------------------|-------|----------------|----------------|----------------|
| <i>Cross section AA'</i> | | | | |
| TS1 | 1A | 1.00 | 1.00 | 1.00 |
| | 2A | 0.96 | 1.03 | 0.98 |
| TS2 | 1A | 1.09 | 0.77 | 0.83 |
| | 2A | 0.96 | 1.02 | 0.83 |

important urban density (i.e. TA2 in Fig. 3c) determines an increasing of the response spectrum, in the period range 0.0–0.2 s, up to 20%. The presence of one building on the right side of the model (TA1) induces a significant increasing of the normalized response spectrum at point 2A in AA' (Fig. 7 right) and not in 1A. The addition of the other buildings in model TA2 leads to an increasing of the response spectrum at both point 1A and 2A due to the generation of multiple radiated wave fields.

To quantify the influence of the urban field on local seismic response in the Fosso di Valerano valley, the amplification factors (AF) is computed as the ratio between the integral of the response spectra in the period bands 0.1–0.5 s, 0.4–0.8 s and 0.7–1.1 s (Tab. 3) and the integrals in the same period bands of free field response spectrum. These proxies allowed to quantify the variation of local seismic response in SCI condition with respect to the free field one. It is worth noticing that the buildings are able to modify the AF values up to 0.2 with respect to free field conditions; such a variation is significant as it was considered as a threshold value for distinguishing seismic microzones in the seismic microzonation studies of level 3 performed in Central Italy after the 2016 seismic sequence (Pergalani et al. 2019). These findings demonstrate that SCI may be a significant contribution to the local seismic response in an urban field where the natural complexity of the geological setting is taken into account for the numerical modelling.

8.3 Spatial variability of ground motion from perturbed wave-field

To highlight the spatial variability of the ground motion due to SCI, the perturbation (U_p) due to the urban wave field is obtained as follows (4):

$$U_p = U_{SCI} - U_f \tag{4}$$

In which U_{SCI} is the urban displacement field at each point along the surface and U_f is the free-field displacement at the same points.

The analysis of U_p along the AA' coupled models (Fig. 8) confirms the strong spatial variability due to the presence of the city. Significant perturbations can be detected in the case of SCI-based models. In case of AA' models, the wave field radiated from a single building clearly appears in Fig. 8a (building 1 in TA1). It is hidden, or combined in a 'group effect', when other buildings are added (buildings 2-3-4 in TA2—Fig. 8b). It is worth noticing that in the AA' case, a unique wave field radiated by the entire city was not detected in TA2 (Fig. 8b). This effect is due to the low urbanization density of TA2. The urban discontinuity that affect the central part of the section (not urbanized area between buildings 1-2-3-4 and 5-6 in TA2) perturbrates the generation of a unique wave field radiated from the city and at least 2 distinguished wave fields can be detected (the first due to buildings 1-2-3-4 and the second to 5-6 in TA2). The density of the city, in terms of presence/absence of urban discontinuities, seems to have a strong role in the number and the typology of the radiated wave fields. Based on these results, the analysis of the perturbed wave fields (Fig. 8) indicates that the presence of buildings induces a strong spatial variability of the ground motion influencing the local seismic response of the entire valley, i.e. not only the areas close to the buildings, as an effect of the generation of radiated wave fields.

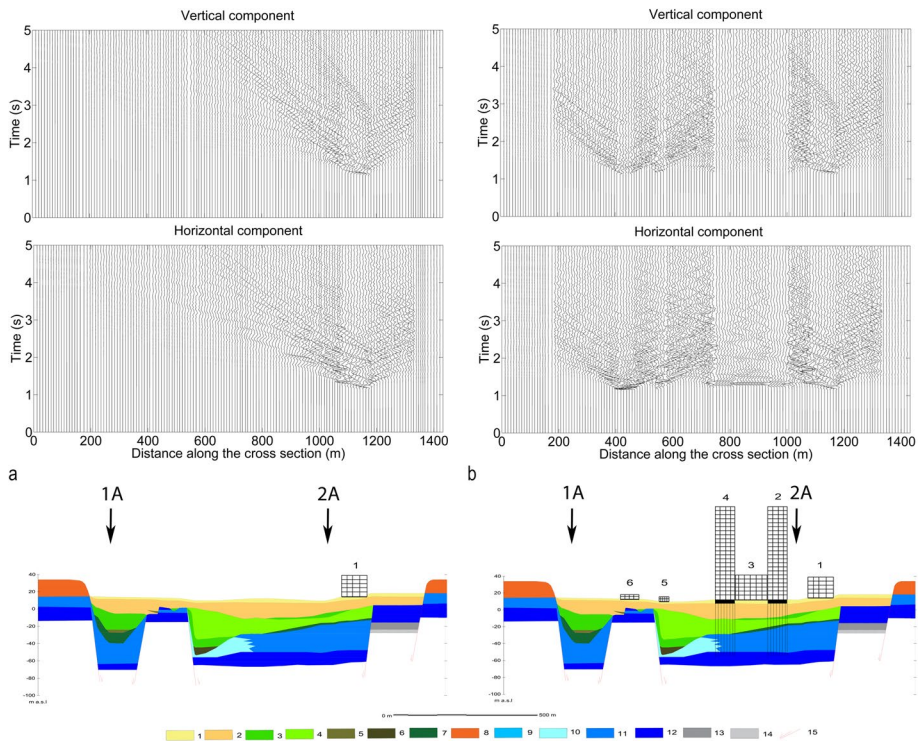


Fig. 8 WPM of the vertical (top) and horizontal (middle) components of the perturbed wave field (in terms of displacement) along the surface of AA' coupled models: TA1 (left), TA2 (right). See Table 1 for geological legend

8.4 Ground heterogeneity and spatial variability of soil properties

To assess the role of the heterogeneities of the alluvial filling, further simulations considering a homogeneous alluvial deposit of the valley were performed. A homogeneous alluvial deposit (soft-soil) composed of AL-CL soil (Table 1) overlying the seismic bedrock (PT-GR in Table 1) was considered. The influence of the soil heterogeneities on the wave field radiated by the buildings was assessed through the differential index ΔU calculated according to (5):

$$\Delta U = |U_{phete} - U_{phomo}| \tag{5}$$

where U_{phete} is the perturbed wave-field (in terms of displacements) obtained considering the heterogeneous alluvial deposits (Fig. 8) and U_{phomo} is the perturbed wave-field (in terms of displacements) obtained when considering a homogeneous alluvial valley. The computed values are interpolated through a Kriging regression and displayed as contour maps under different conditions (Fig. 9). It is possible to notice a strong influence of the heterogeneities on the perturbed wave fields. This influence is stronger for the horizontal component while for the vertical one it seems to be less pronounced. A difference up to 2.2 m is detected in TA2 (Fig. 9) horizontal component while the maximum value for the vertical one corresponds to 1.8 m in TA1 (Fig. 9). Focusing on the horizontal component only, the influence of the heterogeneities persists in the time window (from 1.2 s up to 3.5 s). Such an effect is probably due to the presence of the buried tectonic structures (AA' in Fig. 3) that, in case of homogeneous alluvial filling, play a different role in the waves reflections within the valley. It is worth noticing a singularity around 950–1000 m along the models TA1 and TA2 in Fig. 9: in this portion of the domain, the influence of the heterogeneities in the ground motion time history results strongly persistent for both horizontal and vertical

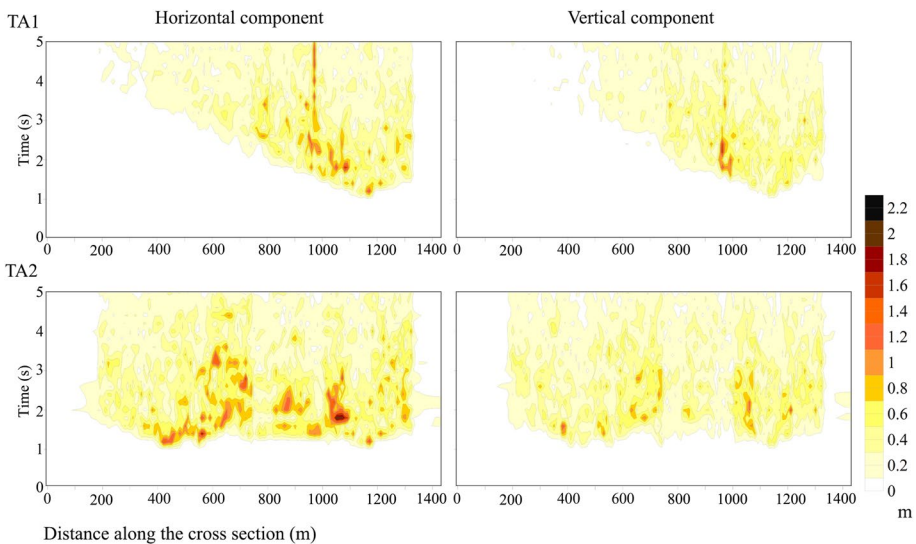


Fig. 9 Contour maps of the ΔU index obtained for the horizontal (left) and vertical (right) components of the perturbed wave field along the surface of AA' coupled models

components. It is likely that this effect can be related to the presence of a thin layer in the heterogeneous model.

9 Conclusion

Through detailed basin and building FEM models, the present results indicate a relevant effect of buildings in modifying the local seismic response with respect to the free-field conditions; this implies a significant variation of wave field characteristics at the free surface based on a Site-City Interaction (SCI) model. The results of this research show that the presence of buildings determines a strong spatial variability of the ground motion. SCI significantly reduces the kinetic energy of the ground motion and the seismic amplification close to the buildings, while these parameters increase in the surrounding areas. Two typologies of effects of SCI could be identified: the first due to the presence of buildings with small volumes and masses (kinematic effect), and the second one by the presence of buildings with large volumes and masses (inertial effect). In both types of interactions, the generated wave field may have affected the ground motion characteristics along the free surface, increasing the amplification values and kinetic energy in the areas surrounding the structures.

Based on these findings, the influence of buildings on the seismic ground motion should not be considered as a local phenomenon only, i.e. due to a single building in a particular position, but as a more widely extended effect due to the urban agglomerate, i.e. due to several buildings that interact one with each other through highly heterogeneous soils. Although differences in the SCI are evident in homogeneous and heterogeneous alluvial deposits, the performed numerical modeling could not distinguish the contributions from the buildings with respect to each single heterogeneity in the SCI. The presence of a single building can modify the response of the site not only locally but also in the whole basin. These results highlight that the urban field influence increases for heterogeneous city agglomerate (i.e. variable in terms of geometry and composition, typologies of foundations, position within the valley) coupled with subsoils characterized by complex geological setting (i.e. heterogeneity of the subsoil deposits and irregular shape of the geological bedrock). Such an effect is clearly showed even though the two-dimensional assumption for soil and structures numerical simulations. Portions of city not yet-urbanized are affected by the presence of buildings in the surroundings so the free field conditions are completely perturbed. Such an evidence is particularly relevant in the framework of urban and land use planning since it is no longer possible to think in terms of local seismic response under free field conditions but a SCI-inclusive perspective should be adopted. To evaluate the seismic ground shaking in case of expanding cities, the analysis of wider areas should be considered to ensure a better constrained urban planning for future buildings at greater distances.

Acknowledgements This study is part of the Ph.D. research of C. Varone on “Vibrational interaction between urban agglomerates and geological system with heterogeneous composition” and was partially funded by a PHC Galileo Project (No. G19-133/42026TH).

Authors' contribution All the Authors contributed to the research design, to the results interpretation and to the manuscript writing; CV and SM performed the engineering-geological modelling and constructed the geological cross-sections; CV, LL and JFS designed the numerical modelling; CV solved the numerical models and processed the outputs. The activities of CV were partly carried out when she was affiliated to NHAZCA S.r.l. Spinoff University of Rome « Sapienza », Via Vittorio Bachelet n.12,00185, Rome, Italy

and to École Supérieure d'Ingénieurs des Travaux de la Construction (ESITC) de Paris - 79, Avenue Aristide Briand, 94110, Arcueil, France.

References


- Alessi D, Bozzano F, Di Lisa A, Esposito C, Fantini A, Loffredo A, Martino S, Mele F, Moretto S, Noviello A, Prestininzi A, Sarandrea P, Scarascia Mugnozza G, Schilirò L, Varone C (2014) Geological risks in large cities: the landslides triggered in the city of Rome by the rainfall of 31 January–2 February 2014. *Ital J Eng Geol Environ*. <https://doi.org/10.4408/ijege.2014-01.o-02>
- Ascani F, Bozzano F, Buccellato A, Del Monte M, Matteucci R, Vergari F (2008) Evoluzione del paesaggio e antiche vie di drenaggio nell'area de "Il Castellaccio" (Roma) da indagini geologiche, geomorfologiche e archeologiche. *Geol Romana* 41:55–77
- Bard PY, Bouchon M (1985) The two dimensional resonance of sediment filled valleys. *Bull Seism Soc Am* 75:519–541
- Bard PY, Chazelas JL, Guéguen P, Kham M, Semblat JF (2005) Site–city interaction. In: Author Oliveira CS, Roca A (eds) *Assessing and managing earthquake risk (geo-scientific and engineering knowledge for earthquake risk mitigation: developments, tools and techniques)*, Springer. ISBN: 1-4020-3524-1:91-114
- Booth DB, Wells RE, Givler RW (2004) Chimney damage in the greater Seattle area from the Nisqually earthquake of 28 February 2001. *Bull Seism Soc Am* 94:1143–1158
- Borchardt RD (1970) Effects of local geology on ground motion near San Francisco Bay. *Bull Seism Soc Am* 60:29–61
- Borchardt RD (1994) Estimantes of site-dependent response spectra for design (methodology and justification). *Earthq Spectra* 10:617–653
- Boutin C, Roussillon P (2004) Assessment of the urbanization effect on seismic response. *Bull Seism Soc Am* 94(1):251–268
- Bozzano F, Caserta A, Govoni A, Marra F, Martino S (2008) Static and dynamic characterization of alluvial deposits in the Tiber River Valley: new data for assessing potential ground motion in the City of Rome. *J Geophys Res* 113:B01303
- Bozzano F, Martino S, Giacomini AC, Lenti L, Martini G, Santisi D'Avila MP (2012) Numerical modeling of nonlinear dynamic shear strains in heterogeneous soils by 1D-3C finite difference SWAP. In: *Proceedings of 15 world conference on earthquake engineering*, September 2012, Lisboa, paper 0427, pp 24–28
- Bozzano F, Marra F, Martino S, Paciello A, Scarascia Mugnozza G, Varone C (2015) The local seismic response of the Fosso di Vallerano valley (Rome, Italy) based on a high resolution geological model. *Rendiconti Online della Soc Geol Ital* 35:29–32
- Bozzano F, Lenti L, Marra F, Martino S, Paciello A, Scarascia Mugnozza G, Varone C (2016) Seismic response of the geologically complex alluvial valley at the "Europarco Business Park" (Rome-Italy) through instrumental records and numerical modelling. *Ital J Eng Geol Environ* 16(1):37–55
- Bozzano F, Buccellato A, Coletti F, Martino S, Marra F, Rivellino S, Varone C (2017) Analysis of the seismic site effects along the ancient Via Laurentina (Rome). *Ann Geophys Italy* 60(4):S0435. <https://doi.org/10.4401/ag-7140>
- Clouteau D, Aubry D (2001) Modification of ground motion in dense urban areas. *J Comput Acoust* 6:1659–1675
- Clouteau D, Ishizawa O, Mezher N (2002) Seismic wave propagation in a random city. In: *7th National conference on earthquake engineering*, Boston
- Colombo C (2012) Prefabbricato e in opera. 120 m in 24 mesi. *Il Nuovo Cantiere*, 6, 16–23 ISSN: 0029-6325 (in italian)
- Dobry R, Vucetic M (1987) Dynamic property and seismic response of soft clay deposits. In: *Proceedings of international symposium on geotechnical engineering of soft soil*, Mexico City, pp 51–87
- Fernández-Ares A, Bielak J (2004) Interaction between earthquake ground motion and multiple buildings in urban regions, Paper S5-4. In: Çelebi M, Todorovska MI, Okawa I, Iiba M (eds) *Proceedings, 3rd UJNR workshop on soil-structure interaction*. Menlo Park, CA, pp 1–11
- Funicello R, Giordano G (2008) Geological Map of Italy 1:50.000, sheet n. 374 'Roma'. Servizio Geologico d'Italia

- Gallipoli MR, Mucciarelli M, Ponzo F, Dolce M, D'Alema E, Maistrello M (2006) Buildings as a seismic source: analysis of a release test at Bagnoli, Italy. *Bull Seism Soc Am* 96:2457–2464
- Gao S, Liu H, Davis PM, Knopoff GL (1996) Localized amplification of seismic waves and correlation with damage due to the Northridge earthquake. *Bull Seism Soc Am* 86:209–230
- Gueguen P, Bard PY (2005) Soil–structure and soil–structure–soil interaction: experimental evidence at the Volvi test site. *J Earthq Eng* 9(5):657–693
- Guéguen P, Bard PY, Oliveira CS (2000) Experimental and numerical analysis of soil motions caused by free vibrations of a building model. *Bull Seism Soc Am* 90(6):2037–2043
- Guéguen P, Bard PY, Chávez-García FJ (2002) Site-city interaction in Mexico city-like environments: an analytical study. *Bull Seism Soc Am* 92(2):794–811
- Hori M, Ichimura T, Wijerathne L, Ohtani H, Chen J, Fujita K, Motoyama H (2018) Application of high performance computing to earthquake hazard and disaster estimation in urban area. *Front Built Environ*. <https://doi.org/10.3389/fbuil.2018.00001>
- Humbert P, Fezans G, Dubouchet A, Remaund D (2005) CESAR-LCPC: a computing software package dedicated to civil engineering uses. *Bull Lab Ponts Chaussée* 256(257):7–37
- Isbiliroglu Y, Taborda R, Bielak J (2015) Coupled soil-structure interaction effects of building clusters during earthquakes. *Earthq Spectra* 31(1):463–500
- Karner DB, Marra F (1998) Correlation of fluvio deltaic aggradational sections with glacial climate history: a revision of the classical Pleistocene stratigraphy of Rome. *Bull Geol Soc Am* 110:748–758
- Karner DB, Marra F, Renne PR (2001) The history of the Monti Sabatini and Alban Hills volcanoes: groundwork for assessing volcanic-tectonic hazards for Rome. *J Volcanol Geoth Res* 107:185–215
- Kham M, Semblat JF, Bard P, Dangla P (2006) Seismic site-city interaction: main governing phenomena through simplified numerical models. *Bull Seism Soc Am* 96(5):1934–1951
- Kumar N, Narayan JP (2018) Quantification of site-city interaction effects on the response of structure under double resonance condition. *Geophys J Int* 212:422–441
- Kumar N, Narayan JP (2019) Quantification of fundamental frequencies of 3D basins and structures and site-city interaction effects on responses of structures. *Pure appl Geophys*. <https://doi.org/10.1007/s00024-019-02158-8>
- Licata V, Forte G, D'Onofrio A, Santo A, Silvestri F (2019) A multi-level study for the seismic microzonation of the Western area of Naples (Italy). *Bull Earthq Eng* 17:4711–4741
- Luco JE, Contesse L (1973) Dynamic structure-soil-structure interaction. *Bull Seism Soc Am* 63:1289–1303
- Marra F, Florindo F (2014) The subsurface geology of Rome (Italy): sedimentary processes, sea-level changes and astronomical forcing. *Earth Sci Rev* 136:1–20. <https://doi.org/10.1016/j.earscirev.2014.05.001>
- Marra F, Bozzano F, Cinti FR (2013) Chronostratigraphic and lithologic features of the Tiber River sediments (Rome, Italy): implications on the Post-glacial sea-level rise and Holocene climate. *Global Planet Change* 107:157–176. <https://doi.org/10.1016/j.gloplacha.2013.05.002>
- Martino S, Lenti L, Gelis C, Giacomini AC, Santisi D'Avila P, Bonilla F, Bozzano F, Semblat JF (2015) Influence of lateral heterogeneities on strong motion shear strains: simulations in the historical center of Rome (Italy). *Bull Seism Soc Am* 105(5):2604–2624
- Meza Fajardo KC, Semblat JF, Chaillat S, Lenti L (2016) Seismic-wave amplification in 3D alluvial basins: 3D/1D amplification ratios from fast multipole BEM simulations. *Bull Seism Soc Am* 106(3):1267–1281
- Meza Fajardo KC, Varone C, Lenti L, Martino S, Semblat JF (2019) Surface waves in a highly heterogeneous alluvial basin: Case study of the Fosso di Vallerano valley, Rome, Italy. *Soil Dyn Earthq Eng* 120:292–300. <https://doi.org/10.1016/j.soildyn.2019.02.008>
- Narayan JP (2010) Effects of impedance contrast and soil thickness on the basin transduced Rayleigh waves and associated differential ground motion. *Pure appl Geophys* 167:1485–1510
- Narayan JP (2012) Effects of P-wave and S-wave impedance contrast on the characteristics of basin transduced Rayleigh waves. *Pure appl Geophys* 169:693–709
- Narayan JP, Kumar V (2014) P-SV wave time-domain finite-difference algorithm with realistic damping and a combined study of effects of sediment rheology and basement focusing. *Acta Geophys* 62(6):1214–1245
- Oñate E (2003) Structural analysis with the finite element method. In: *Linear statics, vol 2, Beams, Plates and Shells*
- Pergalani F, Pagliaroli A, Bourdeau C, Compagnoni M, Lenti L, Lualdi M, Madiari C, Martino S, Razzano R, Varone C, Verrubbi V (2019) Seismic microzonation map: approaches, results and applications after the 2016–2017 Central Italy seismic sequence. *Bulletin of Earthquake Engineering, Special Issue. Seismic Microzonation of Central Italy*. 10.1007/s10518-019-00640-1

- Ricker N (1943) Further developments in the wavelet theory of seismogram structure. *Bull Seism Soc Am* 33(3):197–228
- Ricker N (1953) The form and law of propagation of seismic wavelet. *Geophysics* 18:10–40
- Rovelli A, Malagnini L, Caserta A, Marra F (1995) Using 1-D and 2-D modelling of ground motion for seismic zonation criteria: results for the city of Rome. *Ann Geophys Italy* 38:591–605
- Semblat JF, Pecker A (2009) Waves and vibrations in soils: earthquakes, traffic, shocks, construction works. IUSS Press Istituto Universitario di Studi Superiori di Pavia
- Semblat JF, Dangla P, Kham M, Duval AM (2002) Seismic site effects for shallow and deep alluvial basins: in-depth motion and focusing effect. *Soil Dyn Earthq Eng* 22(9–12):849–854. [https://doi.org/10.1016/S0267-7261\(02\)00107-0](https://doi.org/10.1016/S0267-7261(02)00107-0)
- Semblat JF, Kham M, Bard PY (2008) Seismic-wave propagation in alluvial basins and influence of site-city interaction. *Bull Seism Soc Am* 98(6):2665–2678
- Semblat JF, Lokmane N, Driad-Lebeau L, Bonnet G (2010) Local amplification of deep mining induced vibrations part 2: simulation of ground motion in a coal basin. *Soil Dyn Earthq Eng* 30:947–957
- Semblat JF, Lenti L, Gandomzadeh A (2011) A simple multi-directional absorbing layer method to simulate elastic wave propagation in unbounded domains. *Int J Numer Methods Eng* 85:1543–1563
- Taborda R, Bielak J (2011a) Large-scale earthquake simulation computational seismology and complex engineering systems. *Comput Sci Eng* 13:14–26
- Taborda R, Bielak J (2011b) Full 3D integration of site-city effects in regional scale earth-quake simulations, Paper MS03-241. In: Proceedings, 8th international conference on structural dynamics: EURO-DYN, Leuven, Belgium, pp 511–518
- Tsogka C, Wirgin A (2003) Simulation of seismic response in an idealized city. *Soil Dyn Earthq Eng* 23:391–402
- Ungureanu B, Guenneau S, Achaoui Y, Diatta A, Farhat M, Hutridurga H, Craster RV, Enoch S, Brûlé S (2019) The influence of building interactions on seismic and elastic body waves. *EPJ Appl Metamat* 6:18. <https://doi.org/10.1051/epjam/2019015>
- Varone C, Lenti L, Martino S (2014) Engineering-geological and numerical modeling for the evaluation of the vibrational interaction between the city agglomerate and heterogeneous geological system: preliminary results. In: 33 Conference GNGTS, Bologna (Italy), vol 2, pp 294–301
- Varone C, Lenti L, Martino S (2016) Analysis of earth-quake induced strain effects in a recent urbanized alluvial valley (Rome). *Rendiconti Online della Società Geologica Italiana* 41:354. <https://doi.org/10.3301/ROL.2016.166>
- Wirgin A, Bard PY (1996) Effects of buildings on the duration and amplitude of ground motion in Mexico City. *Bull Seism Soc Am* 86(3):914–920
- Wong HL, Trifunac MD (1975) Two-dimensional, antiplane, building-soil-building interaction for two or more buildings and for incident plane SH waves. *Bull Seism Soc Am* 65:1863–1885

Publisher's Note Springer Nature remains neutral with regard to jurisdictional claims in published maps and institutional affiliations.

Affiliations

C. Varone¹  · L. Lenti^{2,5} · S. Martino³ · J. F. Semblat⁴

¹ CNR - Italian National Research Council, Institute of Environmental Geology and Geoengineering (IGAG), RM1 Via Salaria km, 29, 300-00015 Montelibretti, Italy

² GERS-SRO, IFSTTAR, University Gustave Eiffel, 14-20 Boulevard Newton Cité Descartes, Champs sur Marne, 77447 Marne La Vallée Cedex 2, France

³ Department of Earth Sciences, Research Center for the Geological Risks (CERI), University of Rome «Sapienza», P.za A. Moro 5, 00185 Rome, Italy

⁴ IMSIA, UMR 9219, CNRS-EDF-CEA-ENSTA Paris, Institut Polytechnique de Paris, Palaiseau, France

⁵ CEREMA Méditerranée, Equipe-Projet MOUVGS, Agence Sophia-Antipolis, 500 Route des Lucioles, CS80125, 06903 Valbonne, France